

Small Area Estimation with Spatially Varying Natural Exponential Families

Shonosuke Sugasawa¹, Yuki Kawakubo² and Kota Ogasawara³

¹Center for Spatial Information Science, The University of Tokyo

²Graduate School of Social Sciences, Chiba University

³Department of Industrial Engineering, School of Engineering, Tokyo Institute of Technology

Abstract

Two-stage hierarchical models have been widely used in small area estimation to produce indirect estimates of areal means. When the areas are treated exchangeably and the model parameters are assumed to be the same over all areas, we might lose the efficiency in the presence of spatial heterogeneity. To overcome this problem, we consider a two-stage area-level model based on natural exponential family with spatially varying model parameters. We employ geographically weighted regression approach to estimating the varying parameters and suggest a new empirical Bayes estimator of the areal mean. We also discuss some related problems, including the mean squared error estimation, benchmarked estimation, and estimation in non-sampled areas. The performance of the proposed method is evaluated through simulations and applications to two data sets.

Key words: Empirical Bayes estimation; Geographically weighted regression; Mean squared error; Natural exponential family with quadratic variance function; Small area estimation

1 Introduction

Small area estimation is widely used to produce reliable estimates of areal means with small, or even zero, sample sizes. When area-specific sample sizes are small, it is well recognized that the direct estimator based only on area-specific samples has high variability and is not appropriate for practical use. Hence, we need to “borrow strength” from related areas and produce indirect (model-based) estimates of areal means. To this end, two-stage hierarchical models have been widely used as standard statistical tools in small area estimation. For comprehensive reviews of small area estimation techniques, see Pferffermann (2013) and Rao and Molina (2015).

We suppose we are interested in the true areal mean θ_i for $i = 1, \dots, m$, where m is the number of areas. Let y_i be the direct estimator of θ_i based only on the available samples within the i th area, so that y_i is typically unstable, i.e., the coefficient of variation $\sqrt{\text{Var}(y_i|\theta_i)}/y_i$ is unacceptably large. In order to improve the accuracy of y_i by “borrowing strength” from information on related areas, hierarchical models have been widely adopted. The most common model in small area estimation is a two-stage hierarchical normal model known as the Fay–Herriot (FH) model (Fay and Herriot, 1979), which is applicable for continuous values. For more general cases such as count or binary, models based on a natural exponential family with conjugate priors (Ghosh and Maiti, 2004) or generalized linear mixed models (McCulloch and Searle, 2001; Jiang, 2006) are available. Although such conventional methods do not take account of geographical information, there is a growing body of literature that develops effective methods with use of geographical information. There are mainly two types of the way of adopting geographical information. One is the use of spatial correlated random effects as considered in Bandyopadhyay et al. (2009), Marhuenda et al. (2013), Pratesi and Salvati (2009), Schmid et al. (2016) and Wakefield (2007) among others, and the other is based on geographically weighted regression (Brundson et al., 1996; Fotheringham et al., 2002) as considered in Chambers et al. (2014), Chandra et al. (2012, 2015, 2017) and Salvati et al. (2012) among others.

Although generalized linear mixed models are widely used for non-normal data, it

is well-known that fitting generalized linear mixed models would be computationally intensive due to the intractable integral appeared in the marginal likelihood function. Hence, incorporating spatially correlated random effects or geographical weighted regression into generalized linear mixed models would be computationally burdensome as well, so that it would not be user-friendly. To overcome this difficulty and extend the body of knowledge on this topic, we here focus on models based on the natural exponential family with quadratic variance function proposed in Ghosh and Maiti (2004) and incorporate spatially varying parameters, which is a similar structure used in geographically weighted regression, into the model. We employ the local likelihood method (Tibshirani and Hastie, 1987) to estimate varying parameters, and the bandwidth in the local likelihood is selected via cross validation. The main advantage of the proposed model is the analytical tractability, that is, the marginal likelihood as well as the Bayes estimator in the proposed model can be obtained in a analytical way unlike generalized linear mixed models. Hence, the (local) maximum likelihood estimator and empirical Bayes estimator can be easily computed.

The rest of the paper is organized as follows. In Section 2, we propose spatially varying empirical Bayes methods and discuss some related problems, including mean squared error (MSE) estimation, benchmarked estimation, and estimation in non-sampled areas. In Section 3, we evaluate the finite sample performance of the proposed methods through simulations. In Section 4, we show the results of two applications, the first to Scottish lip cancer data using the Poisson–gamma model and the second to Spanish poverty rate data using the binomial–beta model. Finally, Section 5 discusses the results and concludes the paper.

2 Small area models with spatially varying natural exponential families

2.1 Spatially varying models and local likelihood estimation

Let m be the number of areas; $\{y_i, \mathbf{x}_i\}_{i=1, \dots, m}$ be the sampled data, where y_i is the direct estimator of an area mean μ_i , satisfying $E[y_i | \mu_i] = \mu_i$; and \mathbf{x}_i be a vector of

covariates associated with y_i . Typically, y_i is an unstable estimator of μ_i in the sense that $\text{Var}(y_i|\mu_i)$ is large because of the small sample size within the area. Ghosh and Maiti (2004) proposed the following hierarchical model based on natural exponential family:

$$\begin{aligned} f(y_i|\theta_i) &= \exp \{n_i(\theta_i y_i - \psi(\theta_i)) + c(y_i, \phi_i)\}, \\ \pi(\theta_i; \boldsymbol{\phi}) &= \exp \{\nu(m_i \theta_i - \psi(\theta_i)) + C(\nu, m_i)\}, \end{aligned} \tag{1}$$

where $m_i = \psi'(\mathbf{x}_i^t \boldsymbol{\beta})$ with $\psi'(t) = d\psi/dt$ is the canonical link function, θ_i is a natural parameter, n_i is a known scalar (dispersion) parameter, $\boldsymbol{\phi} = (\boldsymbol{\beta}^t, \nu)^t$ is a vector of unknown model parameters common to all the areas, and $\psi(\cdot)$, $c(\cdot, \cdot)$, and $C(\cdot, \cdot)$ are functions specific to each distribution. For some typical applications, n_i is equal to the sample size within area i . However, in general, n_i is just the dispersion parameter but not necessarily the area sample size. For example, in the application to count data illustrated in Section 4.1, n_i denotes the expected number of the cases of lip cancer in the i th area. Under the model, the area mean μ_i is expressed as

$$\mu_i = \text{E}[y_i|\theta_i] = \psi'(\theta_i),$$

noting that $\text{E}[\mu_i] = m_i$ under (1). Moreover, it is assumed that the conditional variance is a quadratic function of the conditional mean μ_i , namely $\text{Var}(y_i|\theta_i) = n_i^{-1}Q(\mu_i)$, where $Q(x) = v_0 + v_1x + v_2x^2$ for known constants v_0 , v_1 , and v_2 , which are not simultaneously zero.

In this paper, we introduce a spatially varying structures in the model (1), that is, we allow the model parameters in (1) to vary spatially. We propose the following model:

$$\begin{aligned} f(y_i|\theta_i) &= \exp \{n_i(\theta_i y_i - \psi(\theta_i)) + c(y_i, n_i)\}, \\ \pi(\theta_i; \boldsymbol{\phi}(\mathbf{u}_i)) &= \exp \{\nu(\mathbf{u}_i)(m_i(\mathbf{u}_i)\theta_i - \psi(\theta_i)) + C(\nu(\mathbf{u}_i), m_i(\mathbf{u}_i))\}, \end{aligned} \tag{2}$$

where $m_i(\mathbf{u}_i) = \psi'(\mathbf{x}_i^t \boldsymbol{\beta}(\mathbf{u}_i))$, $\mathbf{u}_i = (u_{1i}, u_{2i})$ represent the coordinates of the i th area, and $\boldsymbol{\phi}(\mathbf{u}_i) = (\boldsymbol{\beta}(\mathbf{u}_i)^t, \nu(\mathbf{u}_i))^t$ denote the spatially varying model parameters. Note

that the first-stage model of $y_i|\theta_i$ is the same as (1), while the prior distributions of θ_i are different over the areas. Under the model (2), the Bayes estimator of μ_i under the quadratic loss is given by

$$\tilde{\mu}_i \equiv \tilde{\mu}_i(y_i, \boldsymbol{\phi}(\mathbf{u}_i)) = \frac{n_i y_i + \nu(\mathbf{u}_i) m_i(\mathbf{u}_i)}{n_i + \nu(\mathbf{u}_i)}.$$

Let $\hat{\boldsymbol{\phi}}(\mathbf{u}_i)$ be the estimator of $\boldsymbol{\phi}(\mathbf{u}_i)$ discussed below. Then the empirical Bayes estimator of μ_i can be obtained as $\hat{\mu}_i = \tilde{\mu}_i(y_i, \hat{\boldsymbol{\phi}}(\mathbf{u}_i))$.

To estimate the spatially varying parameters $\boldsymbol{\phi}(\mathbf{u}_i)$, we adopt the local likelihood method (Tibshirani and Hastie, 1987) and estimate $\boldsymbol{\phi}(\mathbf{u}_i)$ by maximizing the following locally weighted log-likelihood function:

$$\ell(\boldsymbol{\phi}(\mathbf{u}_i)) = \sum_{k=1}^m w_b(\|\mathbf{u}_i - \mathbf{u}_k\|) \log M(y_k; \boldsymbol{\phi}(\mathbf{u}_i)), \quad (3)$$

where $w_b(\cdot)$ is a user-specified kernel function with bandwidth b and

$$M(y_k; \boldsymbol{\phi}(\mathbf{u}_i)) = \exp \{C(\nu(\mathbf{u}_i), m_k(\mathbf{u}_i)) - C(n_k + \nu(\mathbf{u}_i), \tilde{\mu}_k(y_k, \boldsymbol{\phi}(\mathbf{u}_i)))\},$$

which is proportional to the marginal likelihood with $m_k(\mathbf{u}_i) = \boldsymbol{\psi}'(\mathbf{x}_k^t \boldsymbol{\beta}(\mathbf{u}_i))$ and

$$\tilde{\mu}_k(y_k, \boldsymbol{\phi}(\mathbf{u}_i)) = \frac{n_k y_k + \nu(\mathbf{u}_i) m_k(\mathbf{u}_i)}{n_k + \nu(\mathbf{u}_i)}.$$

Note that the above function has an analytical form since the function $C(\cdot, \cdot)$ is uniquely and analytically determined by the distribution of θ_i . A common choice of the kernel $w_b(\cdot)$ would be the Gaussian kernel defined as

$$w_b(\|\mathbf{u}_i - \mathbf{u}_k\|) = \exp\left(-\frac{\|\mathbf{u}_i - \mathbf{u}_k\|^2}{2b^2}\right),$$

where b is the bandwidth controlling the rate at which the weight declines depending on the distance between two locations.

In practice, the bandwidth b is unknown and we need to adaptively specify the value. To this end, we use the following cross-validation (CV) criterion based on the

marginal likelihood:

$$\text{CV}(b) = \sum_{i=1}^m \log M(y_i; \hat{\phi}_{(-i)}(\mathbf{u}_i; b)), \quad (4)$$

where $\hat{\phi}_{(-i)}(\mathbf{u}_i; b)$ is the estimates of $\phi(\mathbf{u}_i)$ based on (3) under bandwidth b without using y_i . The optimal b is the maximizer of $\text{CV}(b)$, which can be obtained by using numerical methods. We used the golden section search (Brent et al., 1973) over the interval $[b_\ell, b_u]$, with positive b_ℓ and b_u , for example, $b_\ell = 0.01$ and $b_u = 2 \max_{i,k} \|\mathbf{u}_i - \mathbf{u}_k\|^2$. Finally, the overall estimation procedure is as follows:

Estimation Procedure

1. Decide the bandwidth b by CV criterion in (4).
2. Estimate spatially varying parameter $\phi(\mathbf{u}_i)$ for each area i by maximizing the locally weighted log-likelihood function (3) with bandwidth value decided by step 1.
3. Calculate the empirical Bayes estimates $\hat{\mu}_i = \tilde{\mu}_i(y_i, \hat{\phi}(\mathbf{u}_i))$, where $\hat{\phi}(\mathbf{u}_i)$ is the estimates of spatially varying parameter obtained in step 2.

2.2 Mean squared error estimation

In real-life applications, it is important to measure the uncertainty of the empirical Bayes estimator in order to assess the reliability of the estimates. Traditionally, an estimator of MSEs has been used for this purpose (see Prasad and Rao (1990) and Datta et al. (2005)). The MSE of the empirical Bayes estimator $\hat{\mu}_i$ can be expressed as

$$\begin{aligned} \text{MSE}_i &= \text{E} [(\hat{\mu}_i - \mu_i)^2] = \text{E} [(\tilde{\mu}_i - \mu_i)^2] + \text{E} [(\hat{\mu}_i - \tilde{\mu}_i)^2] \\ &\equiv R_{1i}(\phi(\mathbf{u}_i)) + R_{2i}(\phi(\mathbf{u}_i)), \end{aligned}$$

since $\tilde{\mu}_i = \text{E}[\mu_i|y_i]$. The first term corresponds to MSE of the conditional mean $\tilde{\mu}_i$ given the unknown parameters, thereby we can evaluate $R_{1i}(\phi(\mathbf{u}_i))$ in the same way

as Ghosh and Maiti (2004). Then, it follows that

$$R_{1i}(\phi(\mathbf{u}_i)) = \frac{\nu(\mathbf{u}_i)Q(m_i(\mathbf{u}_i))}{(n_i + \nu(\mathbf{u}_i))(\nu(\mathbf{u}_i) - v_2)},$$

On the other hand, based on the theory of local likelihood (Tibshirani and Hastie, 1987), the estimator $\hat{\phi}(\mathbf{u}_i)$ would converge to the true $\phi(\mathbf{u}_i)$ as $m \rightarrow \infty$. Hence, the difference between $\hat{\mu}_i$ and $\tilde{\mu}_i$ gets negligible as $m \rightarrow \infty$, so that the second term $R_{2i}(\phi(\mathbf{u}_i))$ is expected to vanish as $m \rightarrow \infty$. Hence, we may define $\widehat{\text{MSE}}_i^N = R_{1i}(\hat{\phi}(\mathbf{u}_i))$ as the naive (primitive) estimator of the MSE, which would be consistent under $m \rightarrow \infty$. Although we do not give its rigorous proof, this property will be investigated in simulation studies given in Section 3.3. It is known that, if m is not large, R_{2i} is not necessarily negligible, and the naive estimator could underestimate the true MSE. Moreover, the plug-in estimator $R_{1i}(\hat{\phi}(\mathbf{u}_i))$ is known to have a considerable bias. Therefore, the use of bias-corrected estimator of MSE is a standard approach in the context of small area estimation.

To construct a bias-corrected MSE estimator, we adopt the hybrid bootstrap approach employed by Butar and Lahiri (2003). Let $\{y_1^b, \dots, y_m^b\}$ be the parametric bootstrap samples generated from model (2) with $\phi(\mathbf{u}_i) = \hat{\phi}(\mathbf{u}_i)$, and define $\hat{\phi}^b(\mathbf{u}_i)$ as the estimator computed from the bootstrap samples. Then, the hybrid bootstrap MSE estimator is given by

$$\begin{aligned} \widehat{\text{MSE}}_i^B &= 2R_{1i}(\hat{\phi}(\mathbf{u}_i)) - \frac{1}{B} \sum_{b=1}^B R_{1i}(\hat{\phi}^b(\mathbf{u}_i)) \\ &\quad + \frac{1}{B} \sum_{b=1}^B \left\{ \tilde{\mu}_i(y_i^b, \hat{\phi}^b(\mathbf{u}_i)) - \tilde{\mu}_i(y_i^b, \hat{\phi}(\mathbf{u}_i)) \right\}^2. \end{aligned} \tag{5}$$

Note that the last term corresponds to the estimator of R_{2i} , and first two terms correspond to a bias-corrected estimator of R_{1i} . Here, we use an additive form for bias correction while estimating R_{1i} , although several other forms have been proposed (e.g. Hall and Maiti, 2006).

2.3 Benchmarked estimation

A (weighted) sum of empirical Bayes estimates is not necessarily equal to the corresponding direct estimates, which is not preferable for practitioners. Moreover, the empirical Bayes approach sometimes produces over-shrunk estimates, which results in inaccurate estimates of small area means. To avoid these problems, the benchmarked estimator (Datta et al., 2011; Bell et al., 2013) has been used as a standard tool in small area estimation. Here, we consider the constraint $\sum_{i=1}^m c_i \hat{\mu}_i = \sum_{i=1}^m c_i y_i$ with some known weight c_i satisfying $\sum_{i=1}^m c_i = 1$. A typical choice is $c_i = n_i / \sum_{k=1}^m n_k$. From Datta et al. (2011), the constrained empirical Bayes estimator $\hat{\mu}_i^C$ that minimizes the squared error $\sum_{i=1}^m E[(\hat{\mu}_i^C - \mu_i)^2]$ has the form

$$\hat{\mu}_i^C = \hat{\mu}_i + \omega_i \sum_{k=1}^m c_k (y_k - \hat{\mu}_k), \quad (6)$$

with $\omega_i = c_i / \sum_{k=1}^m c_k^2$. The weight c_i often satisfies $\max_{1 \leq i \leq m} c_i = O(m^{-1})$ like $c_i = n_i / \sum_{k=1}^m n_k$. Then, the difference between $\hat{\mu}_i^C$ and $\hat{\mu}_i$ decreases as the number of areas m increases; namely, the differences are negligible when m is sufficiently large.

Since the benchmarked estimator increases the MSEs compared to the empirical Bayes estimator, we need to assess how large the excess MSE is. Regarding this issue, Steorts and Ghosh (2013) and Kubokawa et al. (2014) investigated the MSE estimators of benchmarked empirical Bayes estimators in area-level models using analytical or numerical methods. Following Kubokawa et al. (2014), we consider a bootstrap method for evaluating the excess MSE. The excess MSE is expressed as

$$\begin{aligned} \text{EMSE}_i &= E [(\hat{\mu}_i^C - \mu_i)^2] - E [(\hat{\mu}_i - \mu_i)^2] \\ &= E [(\hat{\mu}_i^C - \hat{\mu}_i)^2] + 2E [(\hat{\mu}_i^C - \hat{\mu}_i)(\hat{\mu}_i - \tilde{\mu}_i)]. \end{aligned}$$

Therefore, the parametric bootstrap procedure used in the previous section enables us to estimate the excess MSE:

$$\widehat{\text{EMSE}}_i = \frac{1}{B} \sum_{b=1}^B (\hat{\mu}_i^{C,b} - \hat{\mu}_i^b)^2 + \frac{2}{B} \sum_{b=1}^B (\hat{\mu}_i^{C,b} - \hat{\mu}_i^b) \left\{ \hat{\mu}_i^b - \tilde{\mu}_i(\mathbf{y}_i^b, \hat{\boldsymbol{\phi}}(\mathbf{u}_i)) \right\}, \quad (7)$$

where $\hat{\mu}_i^b = \tilde{\mu}_i(y_i^b, \hat{\phi}^b(\mathbf{u}_i))$, and $\hat{\mu}_i^{C,b}$ is the benchmarked estimator (6) by replacing y_i and $\hat{\mu}_i$ with y_i^b and $\hat{\mu}_i^b$, respectively.

2.4 Estimation in non-sampled areas

Real applications could include small areas with zero sample sizes. Let j be the index of a non-sampled area and assume that the covariate \mathbf{x}_j is available. We can define the estimator of μ_j under the spatially varying model (2) as

$$\tilde{\mu}_j(\boldsymbol{\beta}(\mathbf{u}_j)) = m_j(\mathbf{u}_j) = \psi'(\mathbf{x}_j^t \boldsymbol{\beta}(\mathbf{u}_j)), \quad (8)$$

with known $\boldsymbol{\beta}(\mathbf{u}_j)$. The estimator of $\boldsymbol{\phi}(\mathbf{u}_j) = (\boldsymbol{\beta}(\mathbf{u}_j)^t, \nu(\mathbf{u}_j))^t$ can be obtained by maximizing the following local likelihood function:

$$\ell(\boldsymbol{\phi}(\mathbf{u}_j)) = \sum_{k=1}^m w_b(\|\mathbf{u}_j - \mathbf{u}_k\|) \log M(y_k; \boldsymbol{\phi}(\mathbf{u}_j)),$$

thereby we can compute the empirical version of (8).

2.5 Typical Models

We here provide three typical models included in the proposed model (2).

(Fay–Herriot model) When we assume that distributions of $y_i|\theta_i$ and θ_i are both normal, with $n_i = D_i^{-1}$, $\nu(\mathbf{u}_i) = A(\mathbf{u}_i)^{-1}$, $\psi(\theta_i) = \theta_i^2/2$, $v_1 = v_2 = 0$, and $v_0 = 1$, model (2) corresponds to the Fay–Herriot model (Fay and Herriot, 1979) with spatially varying parameters, described as

$$y_i = \mathbf{x}_i^t \boldsymbol{\beta}(\mathbf{u}_i) + \sqrt{A(\mathbf{u}_i)} b_i + \sqrt{D_i} \varepsilon_i, \quad i = 1, \dots, m,$$

where the b_i s and ε_i s are mutually independent standard normal random variables, and the D_i s are known sampling variances. Under the model, the marginal distribution of y_i is also normal, $N(\mathbf{x}_i^t \boldsymbol{\beta}(\mathbf{u}_i), A(\mathbf{u}_i) + D_i)$; thus, the Fisher scoring algorithm is easily implemented for maximizing local likelihood (3).

(Poisson–gamma model) When the distributions of $z_i(\equiv n_i y_i)|\mu_i$ and $\mu_i \equiv \exp(\theta_i)$ are assumed to be Poisson and gamma, respectively, with $\psi(\theta_i) = \exp(\theta_i)$, $v_0 = v_2 = 0$, $v_1 = 1$, and $C(\nu, m) = \nu m \log \nu - \log \Gamma(\nu m)$, model (2) is expressed as

$$z_i|\mu_i \sim \text{Po}(n_i \mu_i) \quad \mu_i \sim \Gamma(\nu(\mathbf{u}_i) m_i(\mathbf{u}_i), \nu(\mathbf{u}_i)), \quad i = 1, \dots, m, \quad (9)$$

where μ_1, \dots, μ_m are mutually independent, $\text{Po}(\lambda)$ denotes the Poisson distribution with mean λ , and $\Gamma(a, b)$ denotes the gamma distribution with density

$$f(x) = \frac{b^a}{\Gamma(a)} x^{a-1} \exp(-bx), \quad x > 0.$$

The model corresponds to the Poisson–gamma model proposed by Clayton and Kaldor (1987) with spatially varying model parameters. It is well-known that the marginal distribution of z_i is a negative binomial distribution with probability function

$$f_m(z_i, \phi(\mathbf{u}_i)) = \frac{\Gamma(z_i + \nu(\mathbf{u}_i) m_i(\mathbf{u}_i))}{\Gamma(z_i + 1) \Gamma(\nu(\mathbf{u}_i) m_i(\mathbf{u}_i))} \left(\frac{n_i}{n_i + \nu(\mathbf{u}_i)} \right)^{z_i} \left(\frac{\nu(\mathbf{u}_i)}{n_i + \nu(\mathbf{u}_i)} \right)^{\nu(\mathbf{u}_i) m_i(\mathbf{u}_i)},$$

and the local likelihood (3) is similar to the likelihood of the geographical weighted negative binomial regression model suggested by Silva and Rodrigues (2014). For maximizing the weighted likelihood (3), we simply employed `optim` function available in R language.

(binomial–beta model) When the distributions of $z_i(\equiv n_i y_i)|\mu_i$ and $\mu_i \equiv \text{logistic}(\theta_i)$ with $\text{logistic}(x) = \exp(x)/(1 + \exp(x))$ are assumed to be binomial and beta, respectively, with $\psi(\theta_i) = \log(1 + \exp(\theta_i))$, $v_0 = 0$, $v_1 = 1$, $v_2 = -1$, and $C(\nu, m) = -\log B(\nu m, \nu(1 - m))$, where $B(\cdot, \cdot)$ denotes beta function, model (2) is expressed as

$$z_i|\mu_i \sim \text{Bin}(n_i, \mu_i) \quad \mu_i \sim \text{Beta}(\nu(\mathbf{u}_i) m_i(\mathbf{u}_i), \nu(\mathbf{u}_i)(1 - m_i(\mathbf{u}_i))), \quad i = 1, \dots, m,$$

where $\text{Beta}(a, b)$ denotes the beta distribution with density

$$f(x) = B(a, b)^{-1} x^{a-1} (1 - x)^{b-1}, \quad 0 < x < 1.$$

This model can be regarded as the extension of the binomial–beta model used by Williams (1975) in terms of the spatially varying hyperparameters. Under the model, the marginal probability function of z_i can be obtained as

$$f_m(z_i, \phi(\mathbf{u}_i)) = \binom{n_i}{z_i} \frac{B(z_i + \nu(\mathbf{u}_i)m_i(\mathbf{u}_i), n_i - z_i + \nu(\mathbf{u}_i)(1 - m_i(\mathbf{u}_i)))}{B(\nu(\mathbf{u}_i)m_i(\mathbf{u}_i), \nu(\mathbf{u}_i)(1 - m_i(\mathbf{u}_i)))},$$

thereby, the weighted likelihood (3) can be maximized by simply adopting `optim` function available in R language.

3 Simulation studies

3.1 Estimation error comparison in sampled areas

We first investigate estimation errors of the proposed estimator with the traditional estimator in finite samples. We consider the Poisson–gamma model described in Section 2.5. As the coordinates $\mathbf{u}_i = (u_{1i}, u_{2i})$ for $i = 1, \dots, m$, we use Scottish lip cancer data used in Section 4. In the dataset, we have $m = 56$ areas. Covariate x_i is generated from the uniform distribution on $(-1, 1)$, which is fixed through simulation run. As the data generating process, we consider the Poisson observation $z_i | \mu_i \sim \text{Po}(n_i \mu_i)$ and for μ_i we consider the following three scenarios:

$$\text{(I) } \mu_i \sim \Gamma(\nu(\mathbf{u}_i)m_i(\mathbf{u}_i), \nu(\mathbf{u}_i)), \quad \nu(\mathbf{u}_i) = 40 \exp(u_{1i} + u_{2i} - 1)$$

$$\text{(II) } \mu_i \sim \Gamma(\nu m_i, \nu), \quad m_i = \exp(0.5 + 0.5x_i), \quad \nu = 40$$

$$\text{(III) } \log \mu_i = \log m_i(\mathbf{u}_i) + b_i, \quad b_i \sim \text{N}(0, 1),$$

with $m_i(\mathbf{u}_i) = \exp\{\beta_0(\mathbf{u}_i) + \beta_1(\mathbf{u}_i)x_i\}$, $\beta_0(\mathbf{u}_i) = u_{1i} - u_{2i} - 1$ and $\beta_1(\mathbf{u}_i) = \sqrt{u_{1i}^2 + u_{2i}^2}$ for scenarios (I) and (III). In each scenario, we divide $m = 56$ areas into 7 groups and set different values of $n_i \in \{5, 10, 20, 30, 40, 60, 100\}$ for different groups.

We apply four models to the simulated data, our proposed spatially varying Poisson–gamma (SVPG) model, SVPG with benchmarking explained in Section 2.3 (SVPG-B), spatially constant Poisson–gamma (SCPG) model and the following Poisson regression with conditional autoregression (PCAR) model (e.g. Escaramis et al., 2008; Goicoa el

al., 2012)

$$z_i | \mu_i \sim \text{Po}(n_i \mu_i), \quad \log \mu_i = \beta_0 + \beta_1 x_i + e_i,$$

where (e_1, \dots, e_m) follows a Gaussian distribution with conditional autoregressive dependencies. Following Ugarte et al. (2014), we used the integrated nested Laplace approximation (Rue et al., 2009) for fitting the PCAR model.

Based on $R = 1000$ simulation runs, we simulate the area-level MSEs, defined as

$$\text{MSE}_i = \frac{1}{R} \sum_{r=1}^R \left(\hat{\mu}_i^{(r)} - \mu_i^{(r)} \right)^2, \quad (10)$$

where $\hat{\mu}_i^{(r)}$ and $\mu_i^{(r)}$ denote the estimated and true values respectively of μ_i in the r th simulation run. Then, we average the area-level MSEs over the same groups of n_i values. To compare the results between four methods, we compute the ratios of averaged MSEs of SVPG, SVPG-B and PCAR methods over averaged MSE of SCPG method. The results are shown in Table 1. Under scenario (I), the proposed SVPG and SVPG-B methods outperform the SCPG method. The improvement of MSE is large especially in the areas for small n_i value. The performance of SVPG and SVPG-B is also better than PCAR except for the group for $n_i = 30$. On the other hand, it is natural for the SVPG and SVPG-B methods to be inefficient compared to the SCPG method under scenario (II) since the former ones use only local information for estimating the hyperparameters. However, it should be pointed out that the difference between the SV and SC methods is quite small in scenario (II) compared to the amount of improvement in scenario (I). Under the scenario (III), in which none of the four models are the true data generating process, SVPG and SVPG-B methods perform the best or the second best. The performance of SVPG and SVPG-B is very similar under all the scenarios. However, benchmarking method is still important for practical use when the model based EB estimates are published by the government to keep consistency of the published values.

Next, we consider the performance of binomial–beta model. For the coordinates \mathbf{u}_i , the auxiliary variable x_i and the known scale parameter n_i , we use the same

values as the simulation for the Poisson observations. As the data generating process, we consider the binomial observation $z_i|\mu_i \sim \text{Bin}(n_i, \mu_i)$ and for μ_i we consider the following three scenarios:

- (I) $\mu_i \sim \text{Beta}(\nu(\mathbf{u}_i)m_i(\mathbf{u}_i), \nu(\mathbf{u}_i)(1 - m_i(\mathbf{u}_i)))$, $\nu(\mathbf{u}_i) = 40 \exp(u_{1i} + u_{2i} - 1)$,
- (II) $\mu_i \sim \text{Beta}(\nu m_i, \nu(1 - m_i))$, $m_i = \text{logistic}(0.5 + 0.5x_i)$, $\nu = 40$,
- (III) $\mu_i = \text{logistic}(\beta_0(\mathbf{u}_i) + \beta_1(\mathbf{u}_i)x_i + b_i)$, $b_i \sim N(0, 0.25)$,

with $m_i(\mathbf{u}_i) = \text{logistic}(\beta_0(\mathbf{u}_i) + \beta_1(\mathbf{u}_i)x_i)$ for scenario (I) and $\beta_0(\mathbf{u}_i) = u_{1i} - u_{2i} - 1$, $\beta_1(\mathbf{u}_i) = \sqrt{u_{1i}^2 + u_{2i}^2}$ for scenarios (I) and (III). We apply four models to the simulated data, our proposed spatially varying binomial–beta (SVBB) model, SVBB model with benchmarking (SVBB-B), spatially constant binomial–beta (SCBB) model and the following logistic regression with conditional autoregression (LCAR) model:

$$z_i|\mu_i \sim \text{Bin}(n_i, \mu_i) \quad \mu_i = \text{logistic}(\beta_0, \beta_1 x_i + e_i),$$

where (e_1, \dots, e_m) follows a Gaussian distribution with conditional autoregressive dependencies.

In the same manner as the Poisson observations, we simulated the area-level MSEs and calculated the ratio of the averaged MSEs over the same groups of n_i values. The results are given in Table 2. We can see that the proposed spatially varying methods work well for the binomial observations as well.

3.2 Estimation error comparison in non-sampled areas

Next, we investigate the estimation errors in non-sampled areas as discussed in Section 2.4. Based on the simulated data in Section 3.1, we omit one area from each group, so that we observe $m = 49$ areas and the last $k = 7$ areas are non-sampled. For the Poisson observations, we compare three methods, SVPG, SCPG and PCAR based on the scenario (I) with $R = 1000$ replications. To compare the results, we simulated the area-level MSEs for $k = 7$ areas based on $R = 1000$ replications and calculated the

ratios of the MSEs of SVPG and PCAR methods over the MSEs of SCPG method. The results are shown in Table 3. From the table, we can see that our proposed SVPG method outperforms SCPG method except for the area with $n_i = 5$. It is noted that PCAR method performs better than SCPG method for 5 out of 7 areas though PCAR performs worse than SCPG under scenario (I) of the simulation in the previous subsection.

For the binomial observations, we compare three methods, SVBB, SCBB and LCAR based on the scenario (I) with $R = 1000$ replications. In the same manner as Poisson observations, we calculated the ratios of the simulated MSEs of SVBB and LCAR methods over the simulated MSEs of SCBB method. The results are given in Table 4, which shows the similar tendency to the Poisson case.

3.3 Finite sample performance of MSE estimators

Finally, we investigate the finite sample performance of the MSE estimators developed in Section 2.2. Like the previous studies, we consider both the Poisson–gamma and binomial–beta models with spatially varying parameters. Both for Poisson and binomial observations, we consider scenario (I) explained in Section 3.1 as the data generating process. The coordinates $\mathbf{u}_i = (u_{i1}, u_{i2})$ were generated from the uniform distribution on $(0, 1) \times (0, 1)$, and covariates x_i , from the uniform distribution on $(-1, 1)$. For the number of the areas m , we consider three situations $m = 30, 50$ and 80 . In each scenario, we divide m areas into 5 groups and set different values of $n_i \in \{10, 15, 20, 25, 30\}$ for the group patterns of n_i .

We first simulate the MSEs (10) based on $R = 1000$ simulation runs, which are used as the true values of the MSE in each area. For estimating these true MSEs, we used estimators given in Section 2.2: the naive estimator $\widehat{\text{MSE}}_i^{\text{N}}$ and the bootstrap estimator $\widehat{\text{MSE}}_i^{\text{B}}$ with $B = 200$ bootstrap samples. Based on $S = 100$ iterations, we calculate the percentage relative bias (RB) and coefficient of variation (CV), which are

respectively defined as

$$\text{RB}_i = \frac{1}{S} \sum_{s=1}^S \frac{\widehat{\text{MSE}}_i^{(s)} - \text{MSE}_i}{\text{MSE}_i}, \quad \text{and} \quad \text{CV}_i = \sqrt{\frac{1}{S} \sum_{s=1}^S \left(\frac{\widehat{\text{MSE}}_i^{(s)} - \text{MSE}_i}{\text{MSE}_i} \right)^2},$$

where $\widehat{\text{MSE}}_i^{(s)}$ is the MSE estimate of the i th area in the s th iteration, and MSE_i is the true MSE value of the i th area.

In Table 5 and 6, RB_i s and CV_i s averaged over the same groups are reported for Poisson–Gamma and binomial–beta model, respectively. From the tables, it can be seen that the naive estimators of the MSE have severe negative bias especially for the case that the number of areas is small. On the other hand, bootstrap estimators can correct the bias even when the number of the areas is small. In addition, for $m = 30$ and $m = 50$ cases, bootstrap estimators have smaller CV than naive estimators. For $m = 80$ case, both methods are comparable in terms of CV since the bias of the naive estimators get smaller because of the large number of areas. It is also observed that RB does not change very much depending on n_i while CV tends to be smaller with larger n_i .

4 Examples

4.1 Scottish lip cancer data

We first apply the proposed method to Scottish lip cancer data collected during the 6 years from 1975 to 1980 in each of the $m = 56$ counties of Scotland. These data were also analyzed by Clayton and Kaldor (1987). The observed and expected number of cases are available for each county, respectively denoted by z_i and n_i . Moreover, the proportion of the population employed in agriculture, fishing, or forestry is available for each county, leading us to use it as covariate AFF_i , following Wakefield (2007). For each area, $i = 1, \dots, m$, we apply the spatially varying Poisson–gamma model:

$$z_i | \mu_i \sim \text{Po}(n_i \mu_i), \quad \mu_i \sim \Gamma(\nu(\mathbf{u}_i) \exp(\beta_1(\mathbf{u}_i) + \beta_2(\mathbf{u}_i) \text{AFF}_i), \nu(\mathbf{u}_i)), \quad (11)$$

where $\mathbf{u}_i = (u_{i1}, u_{i2})$, and u_{i1} and u_{i2} are the standardized longitude and latitude, respectively.

We first search for the optimal bandwidth by minimizing the criteria (4) and arrive at $b^* = 0.900$. Then, we compute the estimates of the hyperparameters as well as the SVEB estimates of μ_i with $b = b^*$, which are shown in Figure 1. According to Figure 1, the hyperparameter estimates change dramatically from area to area. For comparison, we apply the conventional Poisson–gamma model:

$$z_i | \mu_i \sim \text{Po}(n_i \mu_i), \quad \mu_i \sim \Gamma(\nu \exp(\beta_1 + \beta_2 \text{AFF}_i), \nu), \quad (12)$$

and the maximum likelihood estimates of the hyperparameters are $\hat{\nu} = 2.13$, $\hat{\beta}_1 = -0.15$, and $\hat{\beta}_2 = 5.18$.

In order to investigate whether the parameters are spatially varying or not, we calculate the following statistics for each parameter:

$$\frac{\sum_{i=1}^m n_i \{\phi(\mathbf{u}_i) - \bar{\phi}\}^2}{\sum_{i=1}^m n_i}, \quad (13)$$

where $\phi \in \{\beta_0, \beta_1, \nu\}$ and $\bar{\phi} = \sum_{i=1}^m n_i \phi(\mathbf{u}_i) / \sum_{i=1}^m n_i$. The p -value for testing the null hypothesis that there is no spatial variation can be numerically computed via the parametric bootstrap, where the bootstrap samples are generated from the model with spatially constant parameters, that is, (12). The p -values based on 1000 bootstrap samples are 0.096, 0.795 and 0.063 for β_0 , β_1 and ν , respectively. Hence, there could be spatial variations in β_0 and ν whereas there is not so strong evidence for spatial variation in β_1 .

Let $\hat{\mu}_i^{\text{SVEB}}$ and $\hat{\mu}_i^{\text{EB}}$ be the SVEB estimates from (11) and the empirical Bayes (EB) estimates from (12), respectively. In the left panel of Figure 2, we show the sample plot of the percentage relative difference $100 \times (\hat{\mu}_i^{\text{EB}} - \hat{\mu}_i^{\text{SVEB}}) / \hat{\mu}_i^{\text{SVEB}}$ against the log expected number of cases $\log n_i$. We can observe that the differences are larger in areas with small n_i and become smaller as n_i increases. This is because both the SVEB and the EB estimators are close to the direct estimator y_i in areas with large n_i . The right panel of Figure 2 presents the sample plot of the square root of MSE

(RMSE) estimates based on 500 bootstrap samples against $\log n_i$, revealing that the RMSE decreases as n_i increases.

We next compute the benchmarked estimator $\hat{\mu}_i^C$ from (6) with the weight $c_i = n_i / \sum_{k=1}^m n_k$, and the relative differences to $\hat{\mu}_i = \hat{\mu}_i^{\text{SVEB}}$ are presented in the left panel of Figure 3. The figure shows that the differences increase with respect to n_i because of the choice of the benchmarking weight c_i . However, in most areas, the relative differences are smaller than 2%, so that $\hat{\mu}_i^C$ and $\hat{\mu}_i$ are quite similar. Based on 500 bootstrap replications, we calculate the excess MSE estimates using (7) and compute the ratio to the MSE estimates of the SVEB. The histogram of the ratio is given in the right panel of Figure 3, which shows that the percentage of risk inflation is at most 1.4%.

Finally, we assess the performance of non-sampled area prediction. We randomly omit 5 areas and predict μ_i in the omitted areas using SVEB and EB methods. We then compute mean squared distance (MSD) between the predicted values and y_i in the omitted areas. We repeat this procedure for 100 times, and average values of MSD are 0.74 for SVEB and 1.22 for EB, so that SVEB would be more preferable in terms of non-sampled area prediction.

4.2 Spanish poverty rate data

Next, we use the synthetic income data set from Spanish provinces, which is available in R package `sae`. The data set contains unit data for 52 areas. Let $N_i, i = 1, \dots, m$ denote the population sizes of the areas. Let E_{ij} be the equivalized disposable income calculated following the standard procedure of the Spanish Statistical Institute, and z be the poverty line. The poverty rate for area i is defined as $\mu_i = N_i^{-1} \sum_{j=1}^{N_i} I(E_{ij} < z)$. Unfortunately, we do not observe all E_{ij} s but only observe $E_{ij}, j = 1, \dots, n_i$. A direct estimator y_i of μ_i is given by

$$y_i = \frac{1}{n_i} \sum_{j=1}^{n_i} I(E_{ij} < z),$$

where we set z as 0.6 times the median of all the observed income E_{ij} s, following Molina and Rao (2010). As area-level covariates, we use the area-level rates of females and labor, which are respectively denoted by fe_i and lab_i . Since two provinces, PalmasLas and Tenerife, are very far away from the other provinces, we omit their data in this study. Then, we apply the following binomial–beta model for $i = 1, \dots, m$:

$$y_i | \mu_i \sim \text{Bin}(n_i, p_i), \quad \mu_i \sim \text{Beta}(\nu(\mathbf{u}_i)m_i(\mathbf{u}_i), \nu(\mathbf{u}_i)(1 - m_i(\mathbf{u}_i))), \quad (14)$$

where $m_i(\mathbf{u}_i) = \text{logistic}(\beta_1(\mathbf{u}_i) + \beta_2(\mathbf{u}_i)fe_i + \beta_3(\mathbf{u}_i)lab_i)$ and $\mathbf{u}_i = (u_{i1}, u_{i2})$, and u_{i1} and u_{i2} are the standardized longitude and latitude, respectively. For comparison, we also apply the conventional binomial–beta model:

$$y_i | \mu_i \sim \text{Bin}(n_i, p_i), \quad \mu_i \sim \text{Beta}(\nu m_i, \nu(1 - m_i)), \quad (15)$$

with $m_i = \text{logistic}(\beta_1 + \beta_2 fe_i + \beta_3 lab_i)$.

We find that the optimal bandwidth is $b^* = 2.42$. Some empirical quintiles of the hyperparameter estimates are provided in Table 7. Table 7 shows that the median of spatially varying hyperparameter estimates in the spatially varying model (14) is close to the point estimates in the conventional model (15). We also employed the statistics (13) for testing spatial variation, and calculated p -values based on 1000 parametric bootstrap samples, which are also reported in 7. The p -values show that there would be spatial variations in regression coefficients, but there is not so strong evidence for spatial variation in ν .

The left panel in Figure 4 presents the percentage relative difference $100 \times (\hat{\mu}_i^{\text{EB}} - \hat{\mu}_i^{\text{SVEB}}) / \hat{\mu}_i^{\text{SVEB}}$, where $\hat{\mu}_i^{\text{SVEB}}$ and $\hat{\mu}_i^{\text{EB}}$ are the empirical Bayes estimates from (14) and (15), respectively. We can observe that the differences are smaller than 6% in all the areas except one, and they vanish as the area sample size n_i increases. Based on 500 bootstrap replications, we compute the MSE estimates of $\hat{\mu}_i^{\text{SVEB}}$. The RMSE estimates are given in the right panel of Figure 4, showing the natural result that the MSE decreases with respect to n_i . We next compute the benchmarked estimator of p_i in model (14), and we find that the percentage relative difference between the

SVEB and benchmarked estimates are smaller than 0.15%, and the excess risks in benchmarking based on 500 bootstrap samples are negligibly small.

Finally, we assess the performance of non-sampled area prediction. We randomly omit 5 provinces and predict p_i in the omitted areas using SVEB and EB methods. We then compute mean squared distance (MSD) between the predicted values and y_i in the omitted areas. We repeat this procedure for 100 times, and average values of MSD multiplied 100 are 0.55 for SVEB and 0.58 for EB, so that SVEB is slightly better than BB in terms of non-sampled area prediction.

5 Conclusions and discussion

We have developed SVEB methods based on the local likelihood estimation, in which the optimal bandwidth in a kernel function is determined by cross validation. The model we considered can be regarded as a generalization of the two-stage hierarchical area-level models based on a natural exponential family, proposed by Ghosh and Maiti (2004). The model includes the Fay–Herriot model, Poisson–gamma model, and binomial–beta model as special cases, so that it is applicable for continuous, count, and binary data. We considered some problems, including the MSE and benchmarking estimations, as well as estimating in non-sampled areas. The proposed methods were compared with the conventional non-spatial models through simulation and empirical studies. We found that the proposed method works well and improves the estimation accuracy of the traditional methods.

A possible drawback of the proposed method is its computational costs when the number of areas m is large. For a specified bandwidth b , it requires m times maximization of the weighted log-marginal likelihood (3) to compute the hyperparameter estimates in each area, thereby increasing the computational cost linearly depending on m . A possible solution is to assume that m areas can be classified in G groups, where G is much smaller than m , and that the hyperparameters remain the same in all the areas within the same group. This can reduce the number of maximizations from m to G for each b . However, the question remains as to how we may divide the areas efficiently. However, a detailed consideration about this issue exceeds the scope

of this paper, and we leave the problem to a future study.

References

- [1] Bandyopadhyay, D., Reich, B.J. and Slate, E.H. (2009). Bayesian modeling of multivariate spatial binary data with applications to dental caries. *Statistics in Medicine*, **28**, 3492-3508.
- [2] Bell, W.R., Datta, G.S. and Ghosh, M. (2013). Benchmarking small area estimators. *Biometrika*, **100**, 189-202.
- [3] Brent, R. (1973). *Algorithms for Minimization without Derivatives*. Englewood Cliffs N.J. Prentice-Hall.
- [4] Brunsdon, C., Fotheringham, A.S. and Charlton, M. (1998). Geographically weighted regression—modelling spatial non-stationarity. *Journal of the Royal Statistical Society: Series D*, **47**, 431-443.
- [5] Butar, F.B. and Lahiri, P. (2003). On measures of uncertainty of empirical Bayes small-area estimators. *Journal of Statistical Planning and Inference*, **112**, 63-76.
- [6] Chambers, R., Dreassi, E. and Salvati, N. (2014). Disease mapping via negative binomial regression M-quantiles. *Statistics in Medicine*, **33**, 4805-4824.
- [7] Chandra, H., Salvati, N., Chambers, R. and Tzavidis, N. (2012). Small area estimation under spatial nonstationarity. *Computational Statistics & Data Analysis*, **56**, 2875-2888.
- [8] Chandra, H., Salvati, N. and Chambers R. (2015). A Spatially Nonstationary Fay–Herriot Model for Small Area Estimation. *Journal of Survey Statistics and Methodology*, **3**, 109-135.
- [9] Chandra, H., Salvati, N. and Chambers, R. (2017). Small area prediction of counts under a non-stationary spatial model. *Spatial Statistics*, **20**, 30-56.

- [10] Clayton, D. and Kaldor, J. (1987). Empirical Bayes estimates of age-standardized relative risks for use in disease mapping. *Biometrics*, **43**, 671-681.
- [11] Datta, G.S., Ghosh, M., Steorts, R. and Maples, J. (2011). Bayesian benchmarking with applications to small area estimation. *Test*, **20**, 574-588.
- [12] Datta, G. S., Rao, J.N.K. and Smith, D.D. (2005). On measuring the variability of small area estimators under a basic area level model. *Biometrika*, **92**, 183-196.
- [13] Escaramis, G., Carrasco, J.L. and Ascaso, C. (2008). Detection of significant disease risks using a spatial conditional autoregressive model. *Biometrics*, **64**, 1043–1053.
- [14] Fay, R. and Herriot, R. (1979). Estimators of income for small area places: An application of James–Stein procedures to census. *Journal of the American Statistical Association*, **74**, 341-353.
- [15] Fotheringham, A.S., Brunson, C. and Charlton, M. (2002). *Geographically Weighted Regression*. Wiley, West Sussex.
- [16] Ghosh, M. (1992). Constrained Bayes estimation with applications. *Journal of the American Statistical Association*, **87**, 533-540.
- [17] Ghosh, M. and Maiti, T. (2004). Small-area estimation based on natural exponential family quadratic variance function models and survey weights. *Biometrika*, **91**, 95-112.
- [18] Goicoa, T., Ugarte, M.D., Etxeberria, J. and Militino, A.F. (2012). Comparing CAR and P-spline models in spatial disease mapping. *Environmental and Ecological Statistics*, **19**, 573–599.
- [19] Hall, P. and Maiti, T. (2006). On parametric bootstrap methods for small area prediction. *Journal of the Royal Statistical Society: Series B*, **68**, 221-238.
- [20] Jiang, J. (2006). *Linear and generalized linear mixed models and their applications*, Springer, New York.

- [21] Kubokawa, T., Hasukawa, M. and Takahashi, K. (2014). On measuring uncertainty of benchmarked predictors with application to disease risk estimate. *Scandinavian Journal of Statistics*, **35**, 394-413.
- [22] Marhuenda, Y., Molina, I. and Morales, D. (2013). Small area estimation with spatio-temporal Fay–Herriot models. *Computational Statistics & Data Analysis*, **58**, 308-325.
- [23] McCulloch, C.E. and Searle, S.R. (2001). *Generalized, Linear, and Mixed Models*. Wiley, New York.
- [24] Molina, I. and Rao, J.N.K. (2010). Small area estimation of poverty indicators. *Canadian Journal of Statistics*, **38**, 369-385.
- [25] Pfeffermann, D. (2013). New important developments in small area estimation. *Statistical Science*, **28**, 40-68.
- [26] Prasad, N. and Rao, J.N.K. (1990). The estimation of mean-squared errors of small-area estimators. *Journal of the American Statistical Association*, **90**, 758-766.
- [27] Pratesi, M. and Salvati, N. (2009). Small area estimation in the presence of correlated random area effects. *Journal of Official Statistics*, **25**, 37-53.
- [28] Rao, J.N.K. and Molina, I. (2015) *Small Area Estimation, 2nd Edition*. Wiley, New Jersey.
- [29] Rue, H., Martino, S. and Chopin, N. (2009). Approximate Bayesian inference for latent Gaussian models by using integrated nested Laplace approximations. *Journal of the Royal Statistical Society. Series B*, **71**, 319–392.
- [30] Salvati, N., Tzavidis, N., Pratesi, M. and Chambers, R. (2012). Small area estimation via m-quantile geographically weighted regression. *Test*, **21**, 1-28.
- [31] Schmid, T., Tzavidis, N., Münnich, R. and Chambers, R. (2016) Outlier robust small-area estimation under spatial correlation. *Scandinavian Journal of Statistics*, **43**, 806-826.

- [32] Silva, A.R. and Rodrigues, T.C.V. (2014). Geographically weighted negative binomial regression—incorporating overdispersion. *Statistics and Computing*, **24**, 769-783.
- [33] Steorts, R. and Ghosh, M. (2013). On estimation of mean squared errors of benchmarked empirical Bayes estimators. *Statistica Sinica*, **23**, 749-767.
- [34] Tibshirani, R. and Hastie, T. (1987). Local likelihood estimation. *Journal of the American Statistical Association*, **82**, 559-567.
- [35] Wakefield, J. (2007). Disease mapping and spatial regression with count data. *Biostatistics*, **8**, 158-183.
- [36] Williams, D.A. (1975). The analysis of binary responses from toxicological experiments involving reproduction and teratogenicity. *Biometrics*, **31**, 949-952.

Table 1: The ratios of the area-level MSEs of SVPG, SVPG-B and PCAR methods over those of SCPG method. The values are averaged over the groups with the same n_i values.

	n_i	5	10	20	30	40	60	100
Scenario (I)	SVPG	0.880	0.882	0.925	0.847	0.959	0.938	0.992
	SVPG-B	0.880	0.882	0.924	0.847	0.958	0.937	0.993
	PCAR	1.107	0.986	0.973	0.794	1.045	1.042	1.087
Scenario (II)	SVPG	1.010	1.025	1.017	1.026	1.024	1.021	1.020
	SVPG-B	1.010	1.025	1.017	1.026	1.024	1.019	1.019
	PCAR	1.150	1.800	1.277	1.369	1.457	1.592	1.599
Scenario (III)	SVPG	0.959	0.976	1.000	0.993	1.001	1.002	0.998
	SVPG-B	0.959	0.976	0.999	0.993	1.001	1.001	0.998
	PCAR	0.912	0.967	1.011	1.006	1.000	1.009	1.002

Table 2: The ratios of the area-level MSEs of SVBB, SVBB-B and LCAR methods over those of SCBB method. The values are averaged over the groups with the same n_i values.

	n_i	5	10	20	30	40	60	100
Scenario (I)	SVBB	0.961	0.947	0.961	0.926	0.991	0.965	1.002
	SVBB-B	0.961	0.947	0.961	0.926	0.990	0.963	1.004
	LCAR	1.127	1.311	1.115	1.060	1.258	1.273	1.306
Scenario (II)	SVBB	1.013	1.017	1.013	1.012	1.010	1.005	1.007
	SVBB-B	1.013	1.017	1.012	1.012	1.010	1.005	1.007
	LCAR	1.152	1.575	1.302	1.515	1.494	1.721	1.818
Scenario (III)	SVBB	0.976	0.969	0.984	0.971	1.001	0.995	1.004
	SVBB-B	0.976	0.969	0.983	0.971	1.001	0.993	1.006
	LCAR	1.134	1.220	1.099	1.075	1.187	1.149	1.147

Table 3: The ratios of the MSEs for non-sampled areas of SVPG and PCAR methods over those of SCPG method.

n_i	5	10	20	30	40	60	100
SVPG	1.162	0.830	0.780	0.839	0.980	0.622	0.979
PCAR	1.149	0.751	0.906	0.952	1.031	0.694	0.982

Table 4: The ratios of the MSEs for non-sampled areas of SVBB and LCAR methods over those of SCBB method.

n_i	5	10	20	30	40	60	100
SVBB	1.081	0.961	0.932	0.893	0.976	0.888	1.018
LCAR	1.098	0.954	1.002	0.954	0.998	0.939	1.036

Table 5: The relative bias and coefficient of variations of two types of MSE estimators (bootstrap estimator and naive estimator) based on Poisson–Gamma model. The values are averaged over the groups within the same n_i values. RB and RBN denote relative bias of bootstrap estimator and naive estimator, respectively, and CV and CVN denote coefficient of variations of bootstrap estimator and naive estimator, respectively.

	n_i	10	15	20	25	30
$m = 30$	RB	0.091	0.073	0.096	0.035	0.039
	RBN	-0.206	-0.266	-0.189	-0.244	-0.225
	CV	0.581	0.475	0.462	0.401	0.374
	CVN	0.606	0.569	0.487	0.503	0.484
$m = 50$	RB	0.134	0.009	0.085	-0.053	0.09
	RBN	-0.086	-0.277	-0.218	-0.281	-0.171
	CV	0.570	0.476	0.459	0.407	0.404
	CVN	0.521	0.523	0.474	0.487	0.438
$m = 80$	RB	0.153	0.067	0.056	0.075	-0.030
	RBN	0.058	-0.081	-0.120	-0.051	-0.167
	CV	0.607	0.508	0.443	0.408	0.347
	CVN	0.560	0.485	0.419	0.395	0.392

Table 6: The relative bias and coefficient of variations of two types of MSE estimators (bootstrap estimator and naive estimator) based on binomial–beta model. The values are averaged over the groups within the same n_i values. RB and RBN denote relative bias of bootstrap estimator and naive estimator, respectively, and CV and CVN denote coefficient of variations of bootstrap estimator and naive estimator, respectively.

	n_i	10	15	20	25	30
$m = 30$	RB	0.133	-0.019	-0.034	-0.026	-0.049
	RBN	-0.267	-0.400	-0.385	-0.372	-0.409
	CV	0.604	0.429	0.430	0.387	0.340
	CVN	0.580	0.566	0.545	0.534	0.547
$m = 50$	RB	0.157	0.088	0.011	0.004	0.030
	RBN	-0.111	-0.210	-0.282	-0.254	-0.230
	CV	0.593	0.480	0.415	0.375	0.376
	CVN	0.505	0.485	0.476	0.440	0.435
$m = 80$	RB	0.113	0.083	-0.006	0.008	-0.011
	RBN	-0.054	-0.117	-0.226	-0.163	-0.200
	CV	0.615	0.504	0.410	0.375	0.337
	CVN	0.537	0.467	0.440	0.396	0.393

Table 7: Quantiles of hyperparameter estimates in the spatially varying (SV) model and point estimates in the spatially constant (SC) model, and p -values for testing spatial variation using Spanish poverty rate data.

	SV					SC	Spatial variation
	0%	25%	50%	75%	100%	Estimate	p -value
$\hat{\beta}_1$	-7.96	-3.34	-2.28	-1.03	1.11	-2.70	0.052
$\hat{\beta}_2$	-3.47	2.13	3.50	5.26	10.65	3.85	0.065
$\hat{\beta}_3$	-4.54	-2.16	-1.69	-0.90	3.22	-1.19	0.113
$\hat{\nu}$	42.33	44.12	48.06	51.59	103.06	46.32	0.762

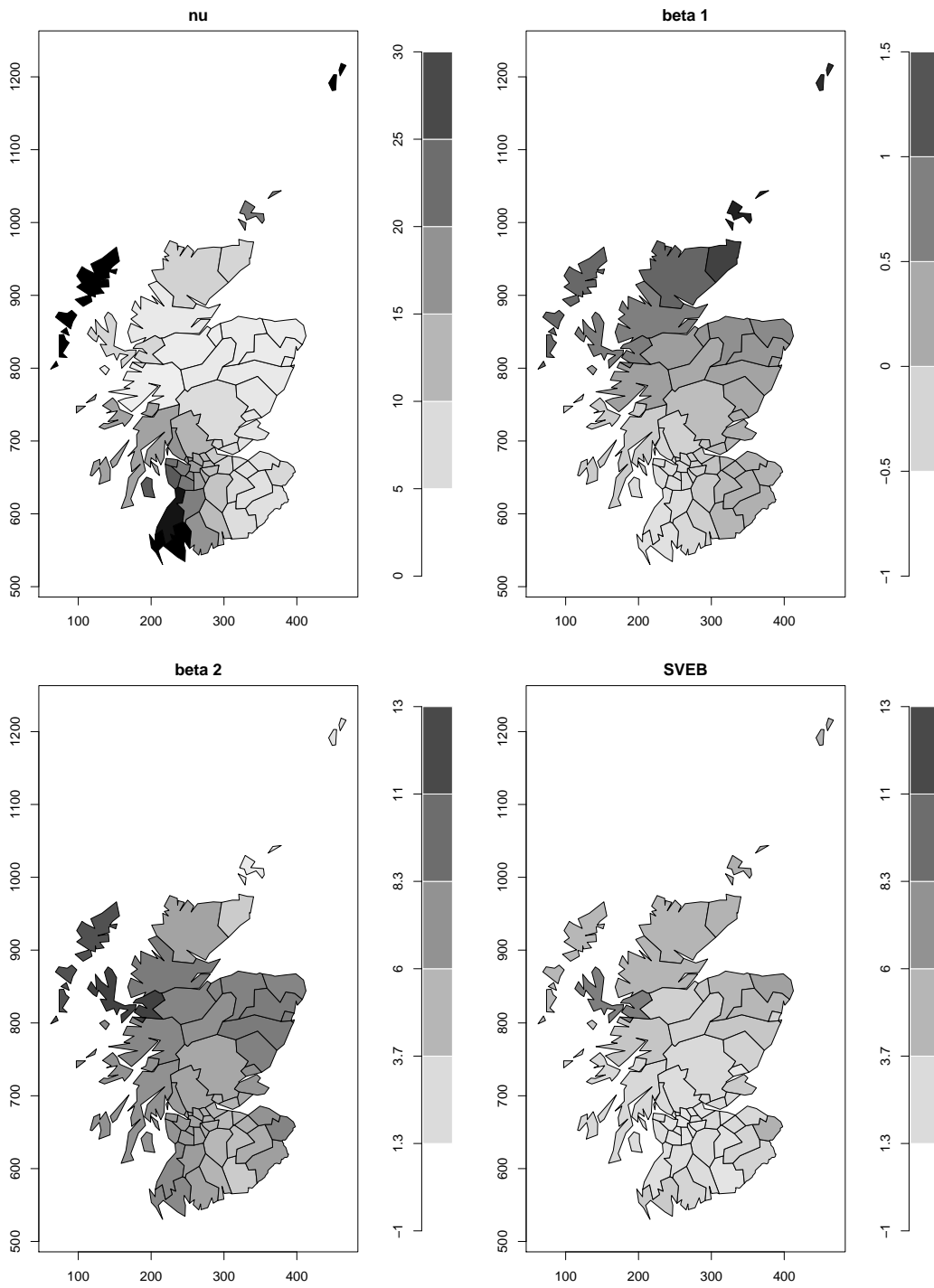


Figure 1: Spatial distributions of $\hat{\nu}(\mathbf{u}_i)$ (top-left), $\hat{\beta}_1(\mathbf{u}_i)$ (top-right), $\hat{\beta}_2(\mathbf{u}_i)$ (bottom-left), and $\hat{\mu}_i$ (bottom-right).

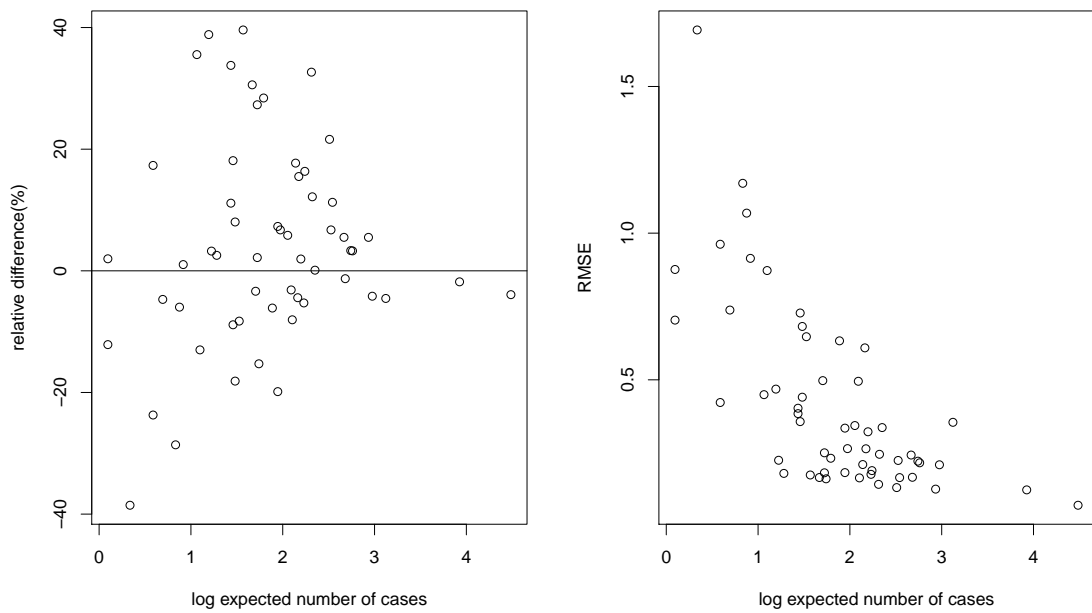


Figure 2: Sample plots of the percentage relative difference between the SVEB and EB estimates: $100 \times (\hat{\mu}_i^{\text{EB}} - \hat{\mu}_i^{\text{SVEB}}) / \hat{\mu}_i^{\text{SVEB}}$ (left) and the squared root of MSE (RMSE) estimates of SVEB against $\log n_i$ (right) using Scottish lip cancer data.

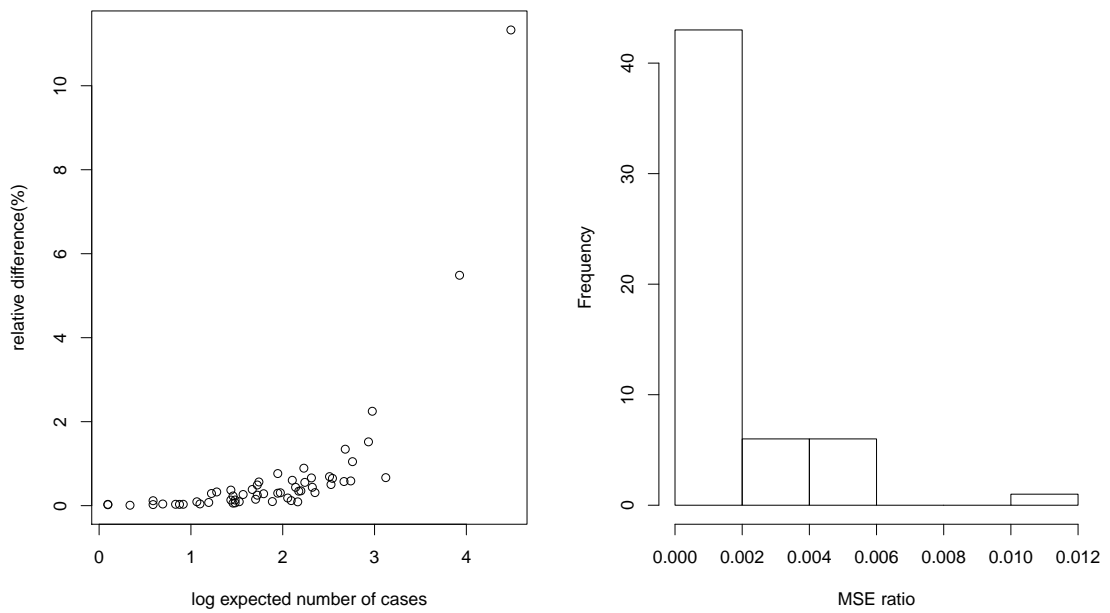


Figure 3: Sample plots of the percentage relative difference between the SVEB and the benchmarked estimators: $100 \times (\hat{\mu}_i^C - \hat{\mu}_i) / \hat{\mu}_i$ (left) and histogram of the excess MSE estimates (right) using Scottish lip cancer data.

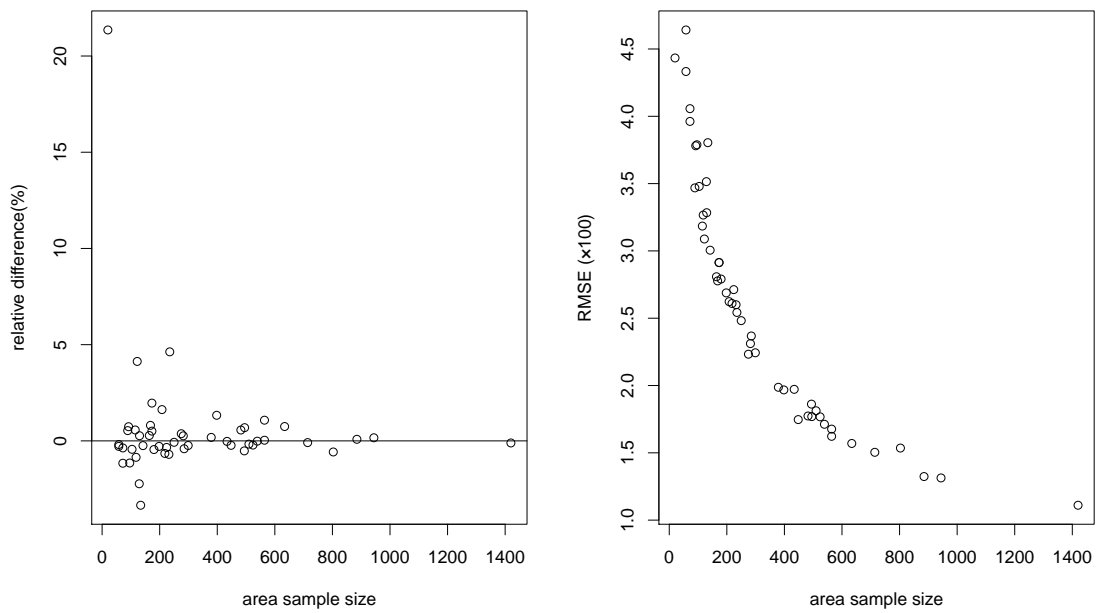


Figure 4: Sample plots of the percentage relative difference between the SVEB and EB estimates: $100 \times (\hat{\mu}_i^{\text{EB}} - \hat{\mu}_i^{\text{SVEB}}) / \hat{\mu}_i^{\text{SVEB}}$ (left) and the squared root of MSE (RMSE) estimates of SVEB against n_i (right) using Spanish poverty rate data.